

Cluster Growth in two- and three-dimensional Granular Gases

S. Miller¹ and S. Luding^{1,2}

¹ Institut für Computeranwendungen 1, Universität Stuttgart,

Pfaffenwaldring 27, D-70569 Stuttgart, Germany

² Particle Technology, DelftChemTech, TU Delft,
Julianalaan 136, 2628 BL Delft, The Netherlands

e-mail: S.Luding@tnw.tudelft.nl

(Dated: February 7, 2020)

Dissipation in granular media leads to interesting phenomena as there are cluster formation and crystallization in non-equilibrium dynamical states. The freely cooling system is examined concerning the energy decay and the cluster evolution in time, both in two and three dimensions. Interesting parallels to percolation theory are obtained in three dimensions.

I. INTRODUCTION

Interesting phenomena can be observed in granular media [1, 2, 3, 4]. The special behavior of granular media is connected to its ability to form a hybrid state between a fluid and a solid: Energy input leads to a reduction of the density due to more collisions and increasing pressure, so that the material can flow, i. e. it becomes “fluid”. On the other hand, in the absence of energy input, granular materials become denser, i. e. they “solidify” due to dissipation. The same coexistence of fluid and solid states also happens without energy input in freely cooling systems. This makes granular media an interesting multi-particle system with a rich phenomenology. However, theoretical approaches are non-classical and appear often extremely difficult, so that there is still active research directed towards the better understanding of granular media.

The subject of this paper is the pattern formation via clustering in a dissipative, freely cooling granular gas [5, 6, 7, 8, 9, 10]. The basic idea of clustering is that in an initially homogeneous freely cooling granular gas, fluctuations in density, velocity, and temperature cause a position dependent energy loss. Due to strong locally inhomogeneous dissipation, pressure and energy drop rapidly and material moves from “hot” to “cold” regions, leading to even stronger dissipation and thus causing the density instability with ever growing clusters until eventually, clusters reach system size (see Fig. 1).

We investigate this clustering instability with respect to different dissipation rates and different system sizes. Furthermore, we attempt to reduce the complexity of the evolution of the examined quantities by simple scaling laws.

In section II, we explain in detail the simulation approach. The results of our numerical experiments are discussed in section III. Finally, in section IV a short summary and a discussion are given.

II. SIMULATION DETAILS

A granular gas can be idealized as an ensemble of hard spheres in which the energy loss that accompanies the

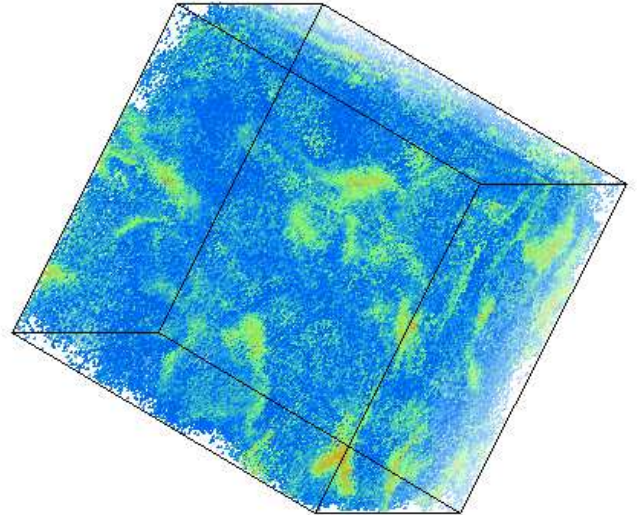


FIG. 1: Snapshot of a 3D system with 512000 particles, volume fraction $\rho = 0.25$, and restitution coefficient $r = 0.3$. The color codes the number of collisions of a particle since the beginning of the simulation. Blue means low number and red means high number of collisions.

collision of macroscopic particles is modeled with a single coefficient of restitution. In the simplest case the particles are identical in size and mass and there are no inter-particle forces between collisions.

Details about initial and boundary conditions are given in section II A. The microscopic dynamics of the motion and the collision of the particles is discussed in section II B and the simulation method is explained in section II C. Section II D deals with the inelastic collapse, a problematic artefact of the hard sphere model with dissipation.

A. Initial and Boundary Conditions

The simulation volume consists of a box with equal side length and periodic boundary conditions in two or three dimensions.

An initial state with random particle positions and velocities is prepared in the following way: The particles first sit on a regular lattice and have a Maxwellian velocity distribution with a total momentum of zero. Then the simulation is started without dissipation and runs for about 10^2 collisions per particle. This state is now used as initial configuration for the dissipative simulations.

B. Microscopic Dynamics

Between collisions no forces act upon the particles and they move at constant velocity.

The particles are idealized as hard spheres. This means that collisions take infinitesimal time and involve only two particles. Conservation of momentum leads to the collision rule [11]

$$\mathbf{v}'_{1/2} = \mathbf{v}_{1/2} \mp \frac{1+r}{2} (\hat{\mathbf{k}} \cdot (\mathbf{v}_1 - \mathbf{v}_2)) \hat{\mathbf{k}}, \quad (1)$$

where a prime indicates the velocities \mathbf{v} after the collision and $\hat{\mathbf{k}}$ is a unit vector pointing along the line of centers from particle 1 to particle 2. The relative tangential velocity does not change during a collision, the relative normal velocity changes its sign and is reduced by the restitution coefficient r . So at each collision, the kinetic energy of the relative velocity's normal component is reduced by the factor $\lambda = 1 - r^2$. The elastic limit $r = 1$ implies $\lambda = 0$, i. e. no dissipation, while $r < 1$ implies $\lambda > 0$.

C. Event-Driven Molecular Dynamics

The simulation of hard spheres can be handled efficiently with event-driven molecular dynamics [12, 13]. The collisions are the events which have to be treated by the algorithm. Between these collisions the particles move on trivial trajectories and so the algorithm can easily compute the point of time t_{12} of the next collision of two particles 1 and 2 as

$$t_{12} = t_0 + \left(-\mathbf{r}_{12} \cdot \mathbf{v}_{12} - \sqrt{(\mathbf{r}_{12} \cdot \mathbf{v}_{12})^2 - (r_{12}^2 - d^2) v_{12}^2} \right) / v_{12}^2, \quad (2)$$

where $\mathbf{v}_{12} = \mathbf{v}_2(t_0) - \mathbf{v}_1(t_0)$ and $\mathbf{r}_{12} = \mathbf{r}_2(t_0) - \mathbf{r}_1(t_0)$ are the relative velocities and positions of the particles at time t_0 , and d is the diameter of a particle.

The algorithm processes the events one after another. After a collision the positions and velocities of the two

involved particles are updated, the state of all other particles remains unchanged. For the two involved particles new events are calculated and the next future event is stored in the event priority queue for both particles. The next event is obtained from the priority queue, the new positions and velocities after the collision for the collision partners are updated, and so on. Neighborhood search is enhanced with standard linked cell methods [14], where the cell change of a particle is treated as a new event type. The details of the algorithm can be found in [12, 13, 15].

D. Avoiding the Inelastic Collapse with the TC Model

Our model makes use of hard spheres with an infinitely stiff interaction potential. This is an idealization of real physical particles and can lead to the dramatic consequence of inelastic collapse: An infinite number of collisions occurs in finite time. This singularity is unphysical, of course, and a major drawback for numerical simulations, too. But it has been shown that one can circumvent this artefact of the model in the following way [16]: If two consecutive collisions of a particle happen within a small time t_c , dissipation is switched off for the second collision. This timestep t_c corresponds to the duration of the contact of physical particles.

There exist other deterministic and random models which prevent inelastic collapse, but most of them lack a solid theoretical background and physical motivation, and since only a small negligible fraction of the particles in the system is involved in the inelastic collapse, these details are insignificant for the physical evolution of the system anyway [16].

III. NUMERICAL EXPERIMENTS

The simulation is started from a homogeneous system, prepared as described in section II A. Depending on the dissipation λ , the density ρ , and the number N of particles, the system remains in the homogeneous cooling regime for some time, until clustering starts and the system becomes inhomogeneous.

We discuss the evolution of the kinetic energy and the collision frequency of the system in section III A. In section III B we investigate the clustering by means of appropriate measures of the cluster size distribution. In section III C we encounter interesting parallels to percolation theory and discuss several critical exponents.

A. Kinetic Energy and Collision Frequency

Dissipative collisions lead to a decay of the kinetic energy and the collision frequency (see Fig. 2 and Fig. 3). From these figures three different regimes can be clearly distinguished. They are:

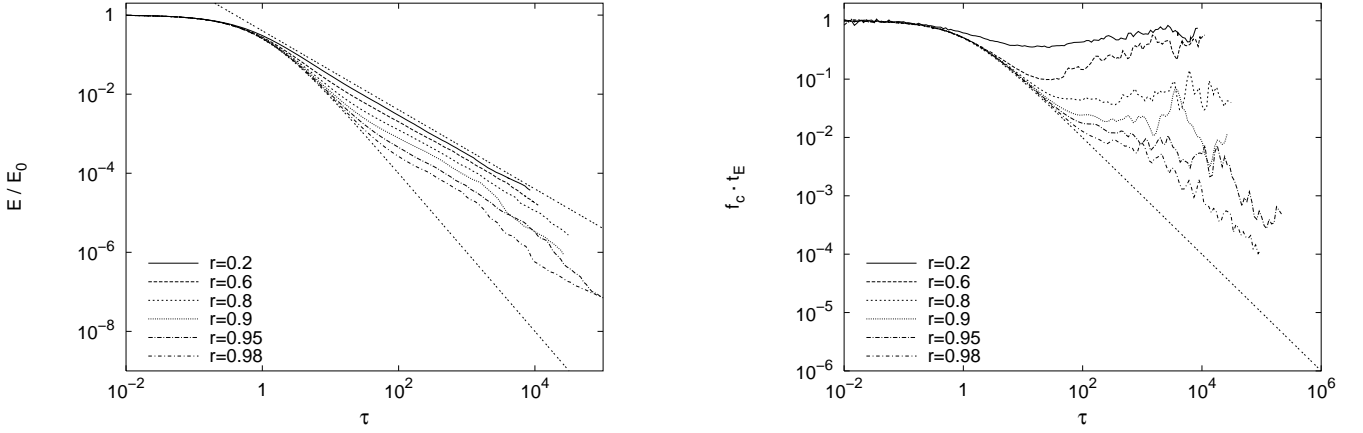


FIG. 2: Decay of the kinetic energy E (left) and the collision frequency f_c (right) plotted against scaled time τ in a 2D system with $N = 316^2 = 99856$ particles, volume fraction $\rho = 0.25$, and different restitution coefficients r . The lines give Eq. 3 and τ^{-1} resp. Eq. 4.

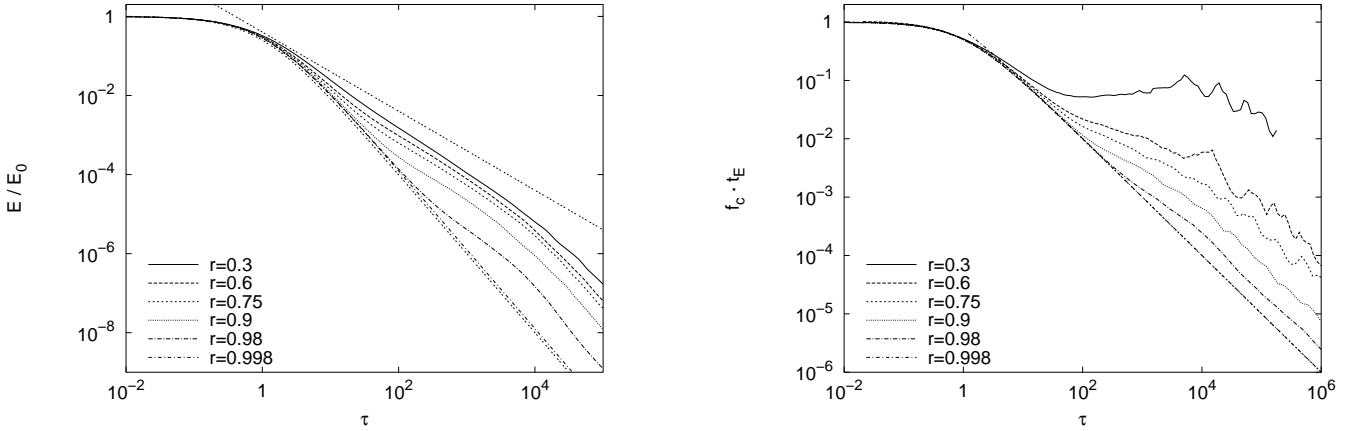


FIG. 3: Decay of the kinetic energy E (left) and the collision frequency f_c (right) plotted against scaled time τ in a 3D system with $N = 80^3 = 512000$ particles, volume fraction $\rho = 0.25$, and different restitution coefficients r . The lines give Eq. 3 and τ^{-1} resp. Eq. 4.

(1) The homogenous cooling regime at the beginning, when no clusters have formed yet, is well understood [17]. The decay of the kinetic energy E is governed by the equation

$$E(\tau) = \frac{E(0)}{(1 + \tau)^2}, \quad (3)$$

with the scaled time $\tau = \frac{\lambda D}{16} \frac{t}{t_E}$. D is the dimension of the system and t_E is the initial Enskog collision time $t_E = (\sqrt{\pi}d)/(2\sqrt{D}v\rho g_d(\rho))$. v is the mean velocity of a particle, d its diameter, ρ is the volume fraction, and g_d is the contact probability. In 2D $g_d(\rho) = (1 - 7\rho/16)/(1 - \rho)^2$ and in 3D $g_d(\rho) = (1 - \rho/2)/(1 - \rho)^3$.

The evolution of the collision frequency per particle

$f_c(\tau)$ with time is given by

$$f_c(\tau) = t_E^{-1}(0) \sqrt{\frac{E(\tau)}{E(0)}}. \quad (4)$$

(2) But when clusters start to grow, the decays deviate from these laws. In this cluster growth regime, the collision frequency fluctuates a lot and the decay of the kinetic energy slows down. The average collision frequency may even increase. The deviation from Eq. 3 occurs earlier and is more dramatic for larger dissipation λ , i. e. smaller r . However, the cluster growth regime is characterized by an energy decay $E \sim \tau^{-1}$, independently of r and D . In contrast, the collision frequency depends on r . This regime is more distinct for large dissipation λ and large system sizes $N^{1/D}$ and can e. g. barely be seen for $r = 0.98$ in Fig. 3.

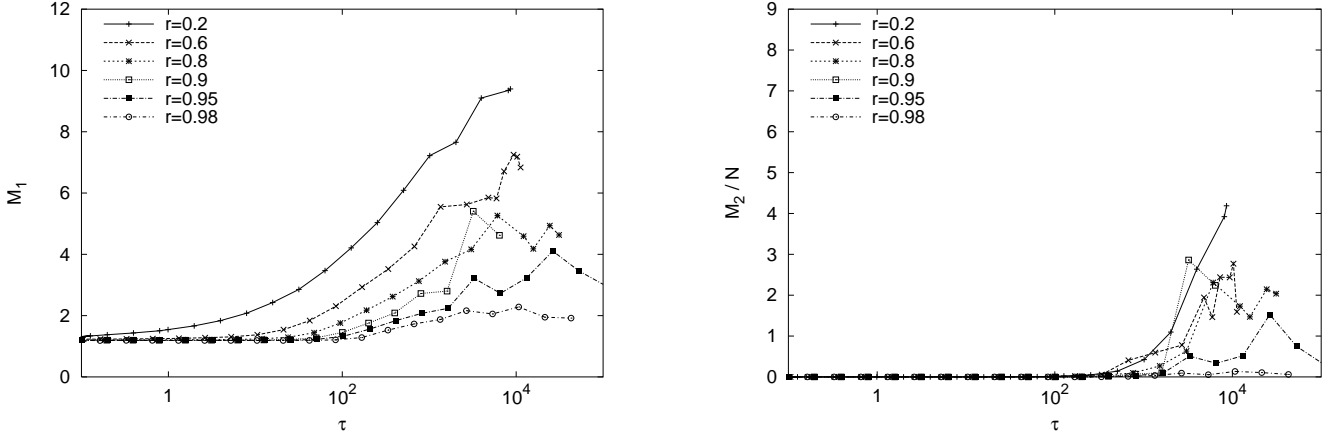


FIG. 4: Growth of the 1st moment M_1 (left) and the 2nd moment M_2 (right) of the cluster size distribution plotted against scaled time τ in a 2D system with $N = 99856$ particles, volume fraction $\rho = 0.25$, and different restitution coefficients r .

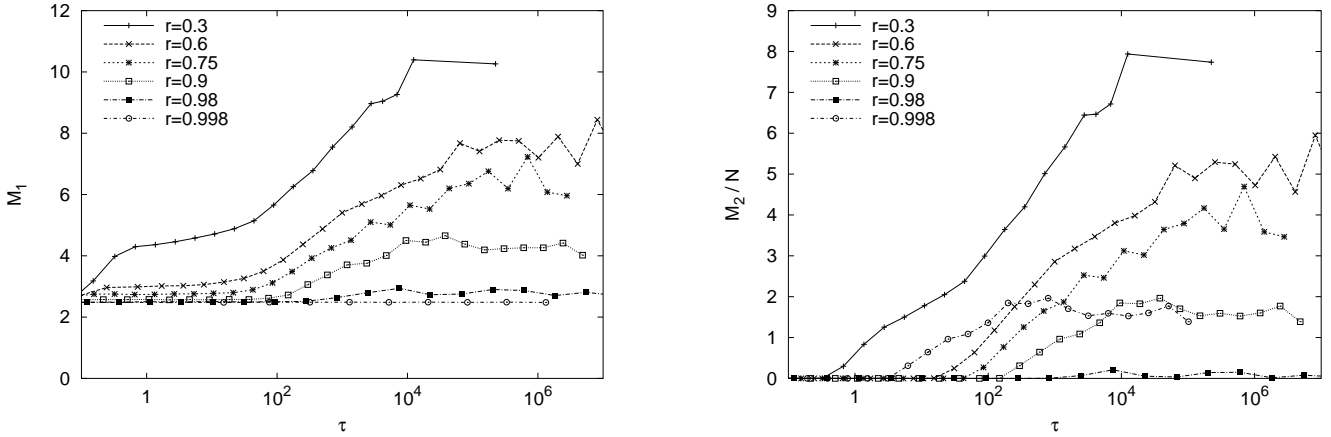


FIG. 5: Growth of the 1st moment M_1 (left) and the 2nd moment M_2 (right) of the cluster size distribution plotted against scaled time τ in a 3D system with $N = 512000$ particles, volume fraction $\rho = 0.25$, and different restitution coefficients r .

(3) Finally, when the largest cluster in the population has reached system size, the cooling resembles to the homogeneous cooling state in so far that $E(\tau) \propto \tau^{-2}$ and $f_c(\tau) \propto \tau^{-1}$, even if the latter still shows large fluctuations.

The 2D situation was discussed in [7, 16] in detail.

B. Cluster Growth

The energy loss of the particles first leads to a reduced separation velocity after collision and eventually to the formation of clusters. But the definition of a cluster suffers from the fact that it takes an infinite number of collisions until the particles could stay in permanent contact with each other [8]. So we use the following definition: Two particles belong to the same cluster, if their distance is smaller than $s = 0.1$ particle diameters. The choice of

s is arbitrary but shifts only the results; the key informations do not depend on s .

The moments M_k of the cluster size distribution are defined as

$$M_k := \frac{1}{n_c} \sum_i i^k n_i, \quad (5)$$

where n_c denotes the total number of clusters and n_i the number of clusters of size i .

In many cases there are a lot of small clusters and one large cluster of size n_x , which contains a macroscopic fraction $m_x := n_x/N$ of the total number N of particles. Therefore, we also define reduced moments M'_k , which do not include the largest cluster.

In Fig. 4 and Fig. 5 the growth of the clusters can be seen on the basis of the first and second moments. After several collisions, particles start to cluster and the moments of the cluster size distribution grow until they

reach their saturation value. A numerical analysis reveals that the increase in M_1 and M_2 is mainly due to one large cluster which grows until it reaches its maximum size. In this final state this cluster contains a macroscopic fraction m_x of the particles (see Fig. 6).

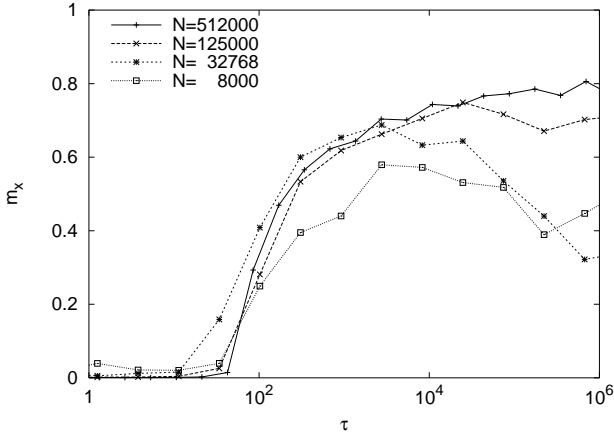


FIG. 6: Growth of the large cluster m_x in a 3D system with N particles, volume fraction $\rho = 0.25$, and a restitution coefficient $r = 0.75$.

The onset time of cluster growth and also the final size m_x of the large cluster depend strongly on the restitution coefficient r (see Fig. 4 and Fig. 5). At low dissipation rates, for a long time nothing interesting happens and finally small and strongly fluctuating clusters appear. High dissipation leads to almost immediate cluster growth and a very large cluster at last. On the other hand, the system size N does not seem to affect the behavior of the system provided that N is not too small (see Fig. 6).

It has been shown [5, 7, 18], that for infinite system size the system is always unstable to the formation of clusters, whereas for a finite system size the density ρ and the dissipation $\lambda = 1 - r^2$ must not be too small. With our choice $N \geq 10^5$ and $\rho = 0.25$ we expect no cluster formation below the critical dissipation $\lambda_c = 10^{-4}$ in our 2D system and $\lambda_c = 10^{-2}$ in our 3D system [7]. This is in good agreement with our results for the 3D system, where cluster formation still can be seen with dissipation $\lambda = 0.04$, but not for $\lambda = 0.0004$ (see Fig. 5).

As can be seen in Fig. 7 (left) the onset τ_c of the growth of the large cluster in 2D does not depend on the restitution coefficient r explicitly. (Implicitly, τ_c is dependent on r via rescaled time, of course.) In contrast τ_c does strongly depend on r in a 3D system (see Fig. 7 (right)). An empirical formula, which gives the dependency rather accurately over orders of magnitude, is

$$\tau_c(\lambda) = 0.28 + 44 \frac{(1 - \lambda)^2}{\lambda} \tau. \quad (6)$$

By rescaling time in Fig. 7 (right) according to Eq. 6, the curves almost collapse, see Fig. 8 (right). In the limit

$\lambda \rightarrow 1$ the time τ_c converges to the constant 0.28, which is equivalent to $3/2 t_E$. This constant stems from the fact that the particles need at least one collision to cluster. In the limit $\lambda \rightarrow 0$ the time τ_c diverges: the particles never start to cluster.

Another difference between the 2D and 3D system in Fig. 7 is the fact that the cluster growth in 2D starts very smoothly, whereas the beginning of the clustering is very sharp in 3D.

C. Critical exponents in 3D

As the moments of the cluster size distribution are clearly dominated by the large cluster, we will now study the reduced second moment M'_2 , which does not include the large cluster. Fig. 9 shows that M'_2 is small most of the time, except for a peak at τ_c . This gives us a clean definition of τ_c . But what is more interesting, parallels to percolation theory arise. In percolation theory [19] one studies the scaling behavior of certain quantities depending on the occupation probability p around the percolation threshold p_c . One result for the reduced second moment $M'_2(p)$ is, e.g.,

$$M'_2(p) \sim |p - p_c|^{-\gamma}, \quad (7)$$

where γ is a universal critical exponent. If we transfer this result to cluster growth, we have to replace p with τ and p_c with τ_c :

$$M'_2(\tau) \sim |\tau - \tau_c|^{-\gamma} \quad (8)$$

Indeed we find in Fig. 9 the same power law behaviour. All data for different system sizes collapse on the same curve and even the exponent $\gamma = 1.8 \pm 0.1$ is in excellent agreement with the 3D percolation problem result $\gamma = 1.80$.

Now, if we study the amplitude of this peak, percolation theory tells us that the maximum sits at

$$p_{max} \sim p_c (1 - aL^{-1/\nu}), \quad (9)$$

where L is the system size, a is a constant, and ν is another critical exponent. Thus we expect:

$$M'_2(p_{max}) \sim L^{\gamma/\nu}. \quad (10)$$

As the system size $L \sim N^{1/3}$, the maximum value of the peak in Fig. 9 scales as

$$M'_{2,max}(N) \sim N^{\gamma/3\nu} \quad (11)$$

Here we can also approve the power law behavior (see Fig. 10). Our simulations yield the result $\gamma/3\nu = 0.77 \pm 0.09$, which leads to $\nu = 0.78 \pm 0.14$. Within the rather large margin of errors this result is close to the 3D percolation problem $\nu = 0.88$, too.

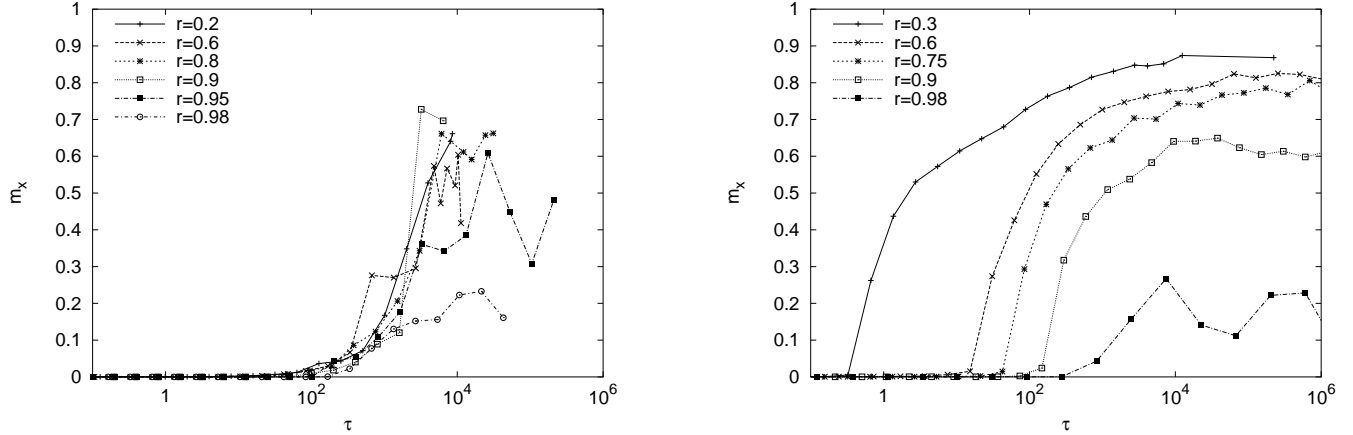


FIG. 7: Growth of the large cluster m_x in 2D (left) and 3D (right) for different restitution coefficients r .

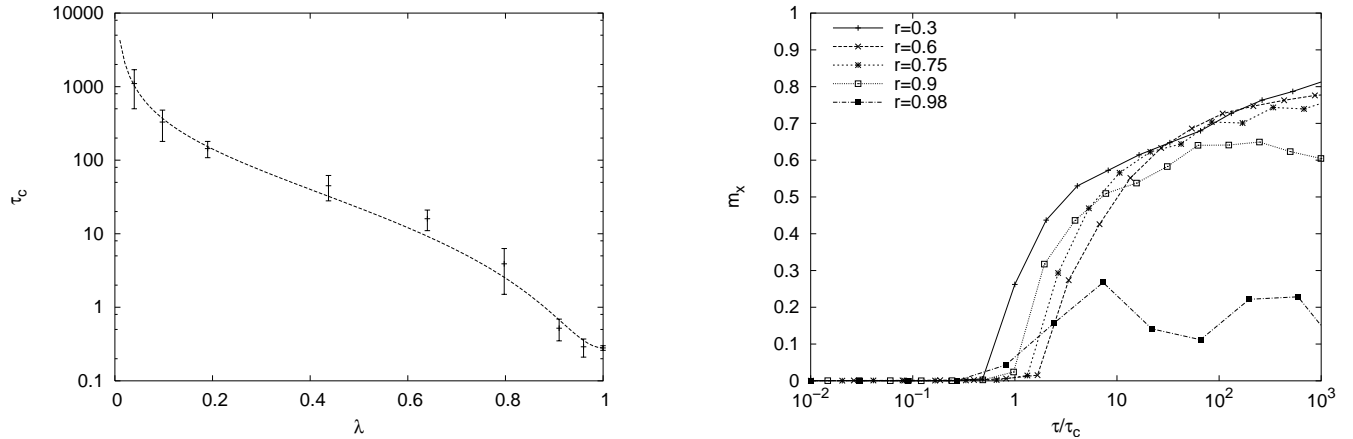


FIG. 8: (left) Scaling behavior of the onset τ_c of the cluster growth in 3D depending on the dissipation rate λ . The dashed curve is Eq. 6.

(right) With rescaled time τ/τ_c according to Eq. 6 the curves of the growth of the large cluster in 3D almost collapse.

IV. SUMMARY AND DISCUSSION

The evolution of freely cooling granular systems can be divided in three regimes.

First, the system is in the homogeneous cooling state. The decay of the kinetic energy E and the collision frequency f_c can be described by the simple analytical expressions $E(\tau) \sim (1 + \tau)^{-2}$ and $f_c(\tau) \sim (1 + \tau)^{-1}$. The time scale is mainly determined by the density and the dissipation rate of the system.

Then clusters begin to develop. The collision frequency shows large fluctuations because of cluster-cluster collisions and cannot be predicted during cluster growth. The energy decay is characterized by $E \sim \tau^{-1}$. This regime shows interesting differences between two and three dimensions. In 3D, cluster growth can be described by a power law behavior with the same critical exponents as in percolation theory. The onset of this cluster growth τ_c is

very sharp and does strongly depend on dissipation λ . In contrast, we could not find a similar behavior in 2D. The onset of the cluster growth is very smooth and depends on dissipation λ only implicitly. In both dimensions the clusters merge to one large cluster which grows until it reaches system size.

When cluster growth has reached a dynamic equilibrium, the system is dominated by one large cluster which contains a macroscopic fraction of the system. Kinetic energy and collision frequency still fluctuate, but are governed by the equations $E(\tau) \sim \tau^{-2}$ and $f_c(\tau) \sim \tau^{-1}$. This means the evolution in time is similar to the homogeneous cooling state.

A very interesting observation is the similarity of clustering in 3D and percolation with respect to the critical exponents. Is this coincidence or is there a deeper reason? We can provide the following explanation: Since the number of particles in our system is fixed, the overall oc-

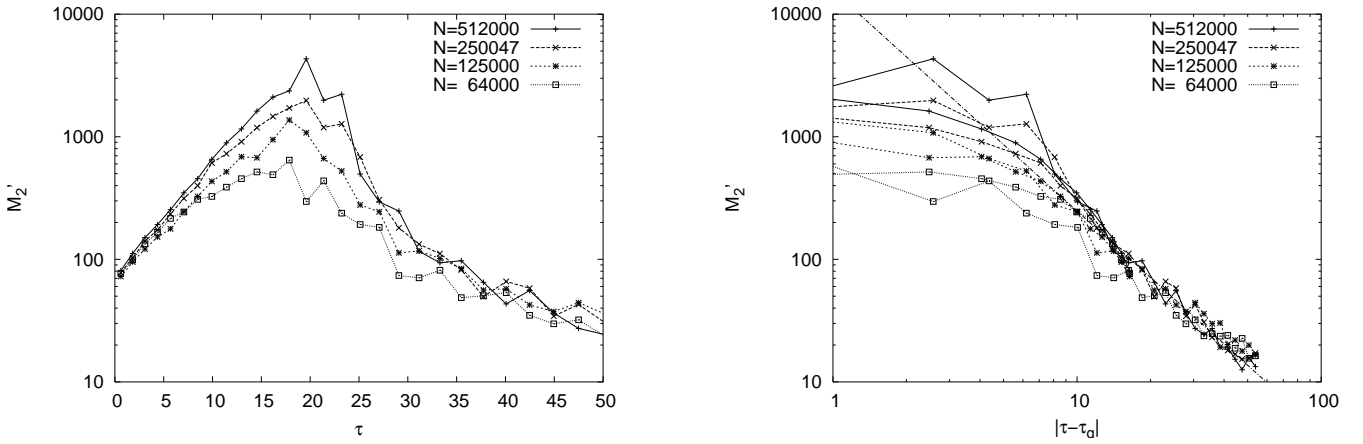


FIG. 9: Reduced 2nd moment M'_2 of the cluster size distribution in 3D systems with different N , volume fraction $\rho = 0.25$, and a restitution coefficient $r = 0.6$. The data are averaged over 10-20 different simulation runs.

(left) The curves show a peak at the onset τ_c of the cluster growth.

(right) Scaling behavior of $M'_2(\tau)$ against $|\tau - \tau_c|$. The dashed curve has a slope of -1.8.

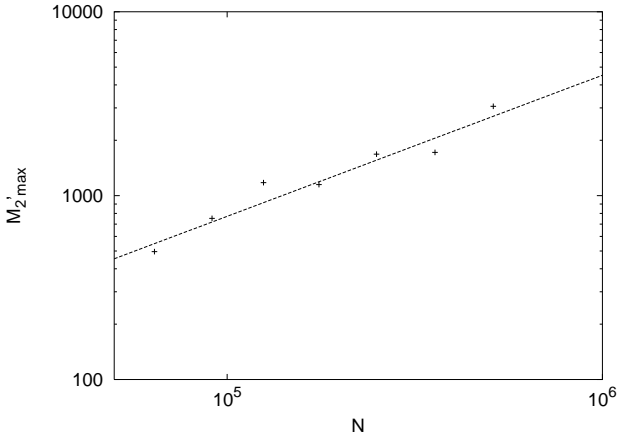


FIG. 10: Maximal amplitude of the reduced 2nd moment M'_2 of the cluster size distribution (see Fig. 9). The dashed curve has a slope of 0.77.

cupation probability is constant, of course. However, the

crucial contribution to the examined quantity M'_2 comes from the clustered regions. The “occupation probability” p in these regions increases with time τ . And fortunately, it even increases linearly (for reasonably small time τ). This can be easily checked if one examines M_1 —an equivalent, but more cleanly defined measure than “occupation probability in clustered regions”. Since there is a linear relation between p and τ , one can be simply replaced by the other without changing the structure of the equations.

In contrast, in our 2D system the growth of the large cluster is much smoother and happens at a very late stage (see Fig. 4 and Fig. 7), when the relation between p and τ is highly non-linear. Thus we could not find universal critical exponents there.

Acknowledgments

This research was supported by the DFG and the SFB 382. We thank Hans Herrmann and Sean McNamara for helpful discussions.

[1] H. J. Herrmann, J.-P. Hovi, and S. Luding, eds., *Physics of dry granular media - NATO ASI Series E 350* (Kluwer Academic Publishers, Dordrecht, 1998).

[2] T. Pöschel and S. Luding, eds., *Granular Gases* (Springer, Berlin, 2001), lecture Notes in Physics 564.

[3] P. A. Vermeer, S. Diebels, W. Ehlers, H. J. Herrmann, S. Luding, and E. Ramm, eds., *Continuous and Discontinuous Modelling of Cohesive Frictional Materials* (Springer, Berlin, 2001), lecture Notes in Physics 568.

[4] Y. Kishino, ed., *Powders & Grains 2001* (Balkema, Rotterdam, 2001).

[5] I. Goldhirsch and G. Zanetti, Phys. Rev. Lett. **70**, 1619 (1993).

[6] I. Goldhirsch, M.-L. Tan, and G. Zanetti, Journal of Scientific Computing **8**, 1 (1993).

[7] S. McNamara and W. R. Young, Phys. Rev. E **53**, 5089 (1996).

[8] S. Luding and H. J. Herrmann, Chaos **9**, 673 (1999).

[9] R. Cafiero, S. Luding, and H. J. Herrmann, Phys. Rev. Lett. **84**, 6014 (2000).

[10] X. B. Nie, E. Ben-Naim, and S. Y. Chen, Phys. Rev. Lett. **89** (2002).

- [11] S. Luding, in *Physics of dry granular media - NATO ASI Series E350*, edited by H. J. Herrmann, J.-P. Hovi, and S. Luding (Kluwer Academic Publishers, Dordrecht, 1998), p. 285.
- [12] B. D. Lubachevsky, *J. Comput. Phys.* **94**, 255 (1991).
- [13] S. Miller and S. Luding (2003), physics/0302002.
- [14] M. P. Allen and D. J. Tildesley, *Computer Simulation of Liquids* (Oxford University Press, Oxford, 1987).
- [15] B. D. Lubachevsky, *Int. J. Comput. Simul.* **2**, 372 (1992).
- [16] S. Luding and S. McNamara, *Granular Matter* **1**, 113 (1998), cond-mat/9810009.
- [17] S. Luding, M. Huthmann, S. McNamara, and A. Zippelius, *Phys. Rev. E* **58**, 3416 (1998).
- [18] N. Sela and I. Goldhirsch, *Phys. Fluids* **7**, 507 (1995).
- [19] D. Stauffer and A. Aharony, *Introduction to Percolation Theory* (Taylor & Francis, London, 1994), 2nd ed.